ChemComm

Support Information

Bismuth Germanate ($Bi_4Ge_3O_{12}$), a Promising High-Capacity Lithium-ion Battery Anode

Received 00th January 20xx,
Accepted 00th January 20xx

DOI: 10.1039/x0xx00000x

www.rsc.org/

Jassiel R. Rodriguez,[a] Carlos Belman-Rodriguez,[b,c] Sergio A. Aguila,[c] Yanning Zhang,[d] Hongxian Liu,[d] and Vilas G. Pol[a,*]

Section 1. Materials and method

Materials Synthesis

$Bi_4Ge_3O_{12}$ (BGO) micropowders were prepared through a sol-gel method using GeO_2 (germanium oxide, 99.99%) and Bi_2O_3 (bismuth oxide, 99.99%) and $C_4H_6O_6$ (L (+)-tartaric acid, 99.5%) as received from Sigma Aldrich. Stoichiometric amounts of germanium and bismuth oxides were dissolved in 50 mL of concentrated nitric acid (70% HNO_3) and stirred at room temperature overnight. Followed by that, 15 mL of a L (+)-tartaric acid solution (0.0171 moles of tartaric acid per BGO gram) was added to the acid mixture and stirred constantly during 3 h. The resultant mixture was heated at 80 °C for another 2 h followed by heated to 100 °C until forming an xerogel. Finally, the resultant powder was annealed at 850 °C for 4h

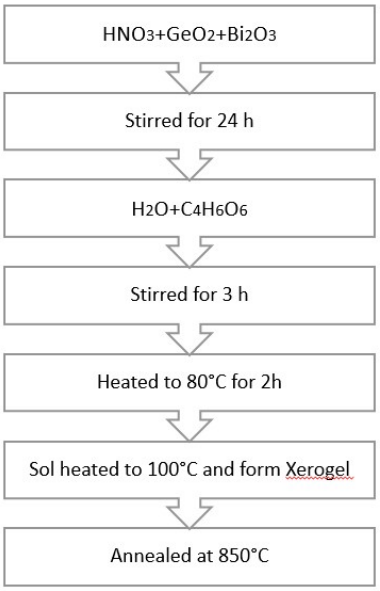

Figure SI1. Flowchart of the synthesis of $Bi_4Ge_3O_{12}$ through a sol-gel precursor method with tartaric acid assistance.

Structure characterization

$Bi_4Ge_3O_{12}$ (BGO) micropowder was analysed by X-ray diffraction (XRD), Scanning electron microscopy (SEM), Transmission electron microscopy (TEM), Infrared and Raman spectroscopies, and N_2 physisorption. using a Philips X'pert diffractometer with a Cu Kα radiation (λ = 1.57 Å), a JEOL JSM 5300 in secondary electron mode, a JEOL JEM-2010 in bright mode, a Nexus-760 FTIR spectrometer with *in situ* Harrick cell, a Thermo-Scientific DXR Raman Microscope with a 633 nm laser and a Quantachrome Nova 2200e surface analyzer at 77K, respectively.

Electrochemical testing

A slurry mixture of 70 wt% BGO, 10 wt% graphene (Sigma Aldrich), 10 wt% carbon Super P (TIMCAL), and 10 wt% CMC (MTI) along with required amount of water were homogeneously mixed. The resultant thick slurry was coated uniformly on a copper foil using a doctor blade method. The coated BGO laminate was dried at 80 °C overnight under vacuum, and then punched into diameter of 12 mm disk electrodes. Then, CR2032 coin cells were assembled, using the prepared electrode as a working electrode, Li metal foil as a counter electrode, and polypropylene film (Celgard 2500) as a separator, in an inert argon-filled glovebox. The electrolyte used was 1 M $LiPF_6$ in EC: DEC with 1: 1 volume ratio. Cyclic voltammetry (CV) analysis were performed between a voltage window of 0.01−3 V *vs* Li/Li^+ at a scan rate of 0.2 mV s^{-1} using Electrochemistry test station Gamry Reference 600. Ccharge-discharge Galvanostatic cycling data were collected from an Arbin BT-2000 Potentiostat.

DFT calculations

DFT (Density functional theory) calculations were achieved using the planewave-based VASP (Vienna ab-initio simulation package). GGA (generalized gradient approximation) method within PBE (Perdew-Burke-Ernzerh) of exchange-correlation functional and PAW (projector augmented wave) potentials were adopted through the work. The kinetic energy cut-off for the plane-wave expansion was established to 520 eV, and the Brillouin-zone integrations for the geometry optimizations were sampled by a (3×3×3) Monkhorst-Pack mesh. The convergence threshold for self-consistent energy error was set to $1x10^{-5}$ eV, and both atomic and lattice parameters coordinates were fully relaxed until the maximum force is smaller than 0.03 eV/Å for each atom.

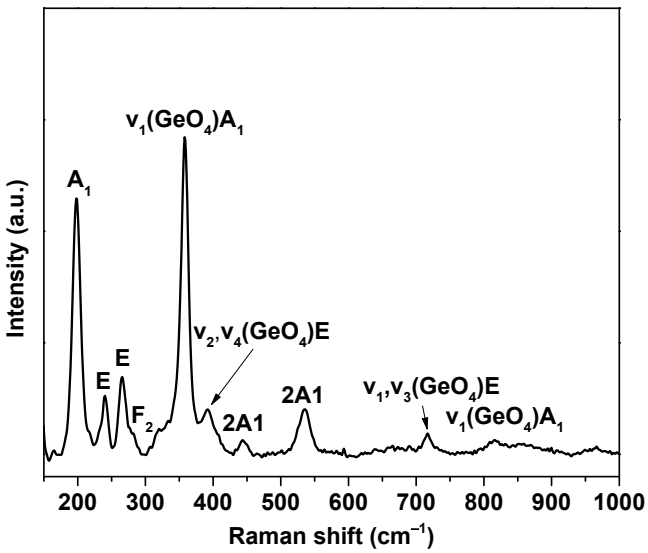

Figure SI2. Raman information of BGO, with its characteristic Raman active modes.

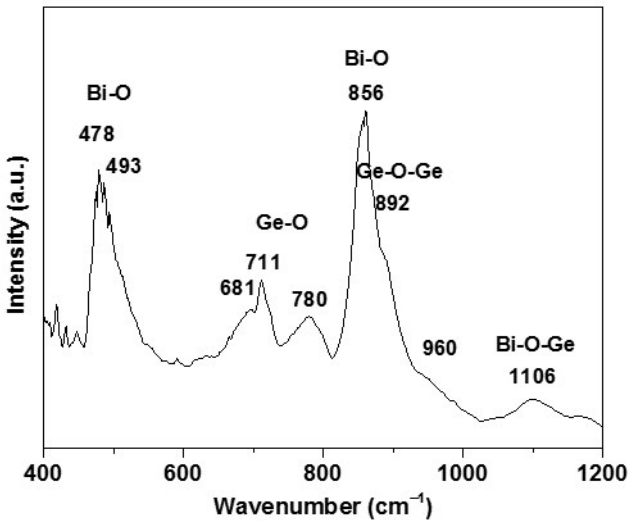

Figure SI3. FT-IR spectra of BGO, with its characteristic FT-IR active modes.

After one charge-discharge cycle, the XRD pattern of BGO pristine material disappeared, indicating that BGO phase transformation through a lithiation reaction is not reversible. The X-ray peaks observed after first C-D cycle at 2θ of 27.2°, 46.0°, and 55.4° correspond to the (201), (222) and (421) planes of the tetragonal crystal system of β-Bi_2O_3, respectively, in agreement with JCPDS PDF 27-0050. Also, The X-ray peaks observed at 2θ of 26.4°, 38.0°, 39.7°, 48.8° and 56.1° correspond to the (101), (102), (111), (112) and (210) planes of the hexagonal crystal system of GeO_2, respectively, in agreement with JCPDS PDF 36-1463. No diffraction peaks of BGO is observed in the XRD pattern, indicating its transformation to other two phases.

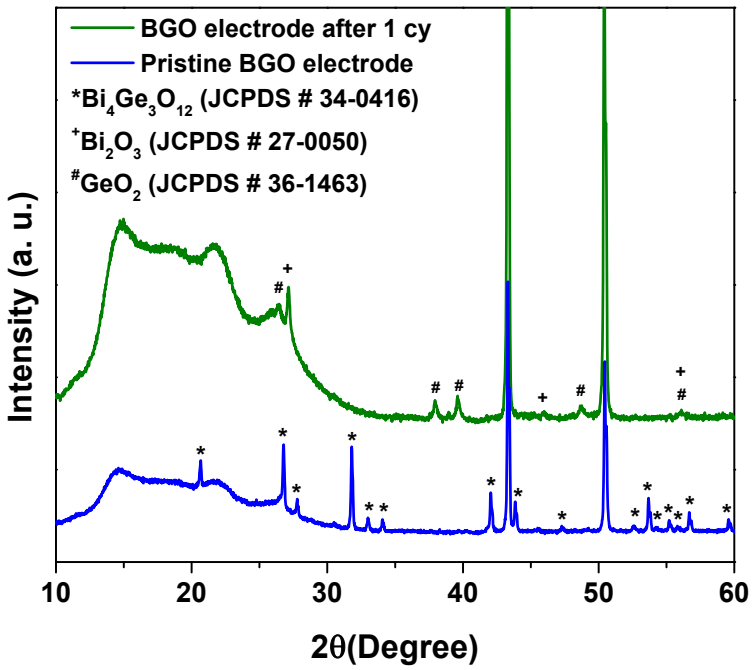

Figure SI4. Ex-situ XRD pattern of BGO anode after first cycle of charge-discharge between 0.01 to 3.0 V vs Li/Li^+.

When one Li atom was put in $Bi_4Ge_3O_{12}$, the structure in the left panel in Fig. SI4 is energetically preferred where Li is surrounded by O atoms. Our preliminary results on the structural stabilities of $Li_xBi_4Ge_3O_{12}$ with high Li compositions reveal the breaking of Bi-O bonds and the appearance of some Bi-Bi bonds with the increasing of Li, such as $Li_6Bi_4Ge_3O_{12}$ in the middle panel. In contrast, the Ge-O bonds (i.e. the green tetrahedra) are hard to be broken in a large *x* range, as shown in the example of $Li_{10}Bi_4Ge_3O_{12}$.

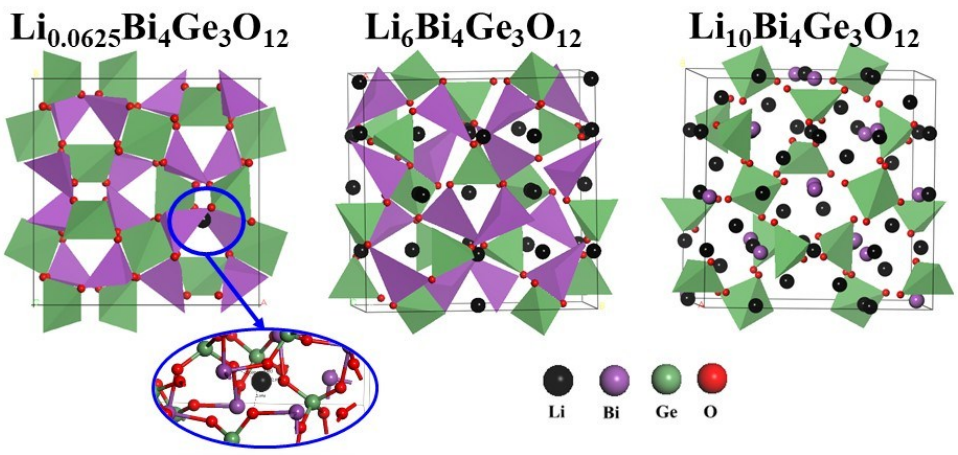

Figure SI5. Simulated insertion of 6 and 10 Li^{+}-ions inside $Bi_4Ge_3O_{12}$ crystal structure.